Solid State Modulator for Plasma Channel Drilling

J. Biela, C. Marxgut, D. Bortis and **J. W. Kolar**
Power Electronic System Laboratory, ETH Zurich
Physikstrasse 3
8092 Zürich, Switzerland

ABSTRACT

In addition to conventional drilling and demolition techniques, drilling with pulsed electric power has been investigated intensively, and commercial applications have begun to emerge. The most efficient method, often called plasma channel drilling (PCD), uses electrical pulses to generate a plasma channel in the rock. The expansion of this channel within the rock performs the demolition. The technique relies on that fact that for fast pulse rise-times (50 ns - 500 ns) the breakdown field-strength of water is higher than that of rock, so that the discharge takes place in the rock. To date, in publications dealing with this topic, plasma dynamics, crack formation, and setup of the electrodes are the primary areas of investigation. In these investigations, the high voltage pulses have been generated using modulators based on spark gaps: either as single-switch or in a Marx-generator setup. These modulators are able to generate high voltages and high currents simultaneously, but the PCD method does not require high currents for igniting the discharge. Meanwhile, after ignition the voltage across the arc is relatively small. Thus these modulators are oversized. In this paper, a new concept, consisting of a solid state modulator which generates a high-voltage pulse for ignition, and a high output-current to expand the plasma, is presented. The solid state modulator consists of a single semiconductor switch, saturable inductors and a pulse transformer. In addition to being more compact, the solid state approach has improved lifetime and reliability compared to approaches using spark gap switches.

Index Terms — **Solid State Modulator, Plasma Channel Drilling**

1 INTRODUCTION

IN addition to conventional mechanical and explosive drilling and demolition of rocks, drilling based on the use of pulsed electric power has been the subject of intense investigation [1, 2] and commercial applications have begun to emerge [3-6], motivated by the relatively low specific energy consumption (cf. Table 1). This method feeds high-voltage pulses, with durations in the microsecond range, to electrodes which are close to, or in contact with, the rock (Figure 1). The electrodes and the rock are usually in a liquid dielectric (typically water). The high-voltage pulse between the electrodes induces a dielectric breakdown, which shatters the rock. Depending on the location of the breakdown, two different effects are used for crushing/drilling the concrete/rock. In the first, a discharge in the dielectric/water outside the rock is generated. This excites a sonic impulse/pressure wave which breaks the surface of the rock/concrete [4].

A more efficient approach, often called Plasma Channel Drilling (PCD) [7], utilizes the fact that for fast pulse rise-times (50 ns - 500 ns) the breakdown field-strength of water increases more rapidly than that of stone (Figure 2). This results in breakdown within the rock rather than in the dielectric for sufficiently fast pulse-edges [1, 2]. This effect is explained in [8] by the breakdown of gas cavities inside the rock.

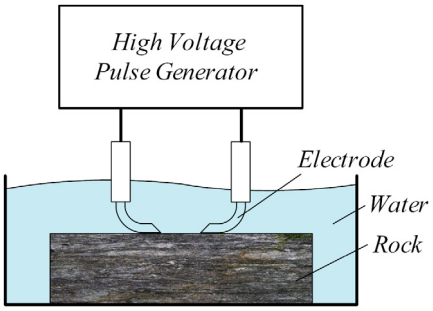

Figure 1. Basic setup for PCD consisting of a pulse modulator generating a high voltage and a high current pulse, two electrodes, a dielectric, and a rock.

The expanding plasma channel inside the rock causes a pressure wave, which disintegrates the material from inside. Due to the direct impact, this is more efficient than breakdown in the liquid, particularly because it is difficult to focus the sonic impulses caused by the breakdown in the direction of the material.

In [2] and other publications, the discharge plasma dynamics, the crack formation, and the final destruction have been studied in detail. Different arrangements and shapes of electrodes have been proposed and tested experimentally. In [7] and in [9] for example

Manuscript received on 30 September 2008, in final form 11 June 2009.

Table 1. Energie consumption of different drilling methods [8, 9, 11-13].

Method	Specific Energy [J/cm^3]
Rotary Drilling	600 - 950
Percussion Drilling	200 - 650
Percussion-Rotary Drilling	400 - 800
Electro Thermal Drilling	5.000
Electro Hydraulic Drilling	400 - 500
Electric Discharge Machining	~ 10.000
Plasma Channel Drilling	100 – 200

coaxially shaped electrodes are investigated, and in [10] rod electrodes with an L-bend are used to drill a slot into a rock. Electric discharge drilling is also used in mining machines in conjunction with mechanical chisels [6].

Thus far no investigations have been performed to optimize the power modulator for PCD, and the high voltage pulse has been generated with modulators based on spark gap switches, either in a single switch configuration or as a Marx generator, to increase the pulse voltage. These modulators are able to generate high voltages and high currents at the same time, but the PCD method requires the high voltage only to ignite the discharge. After ignition the voltage across the load is relatively small, even for load currents in the kA range. This is because the resistivity of the arc is usually well below1 Ω, typically some 10 mΩ, as seen in the voltage and current waveform diagrams in the previously cited publications. As a consequence, the applied pulse modulators are much larger than necessary. Furthermore, the spark gaps are unreliable and have limited life times.

To address these concerns, a compact solid state modulator which generates a high voltage pulse for ignition, and thereafter a high output current, is presented in this paper. The modulator consists of a single semiconductor switch, two capacitors, two saturable inductors and a pulse transformer for generating the ignition voltage. The schematic and the operation principle of the proposed modulator are presented in section 2. Section 3 discusses the mechanical construction of a prototype system, and section 4 presents results for the ignition voltage at the electrodes and the current through the plasma/arc.

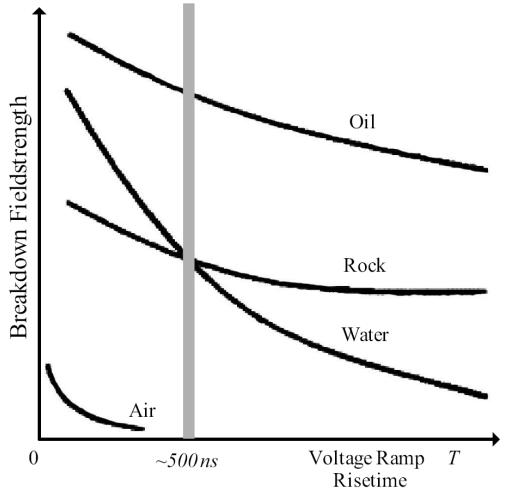

Figure 2. Breakdown voltage of water, air and rock as function of the rise-time of the voltage pulse [3].

2 PULSE MODULATOR

For the PCD a high pulse voltage is required to ignite the electric arc. After ignition a high current is needed to generate a high pressure in the discharge channel for disintegrating the rock. In the past these conditions have been generated using modulators based on spark gap switches, which provide a high blocking voltage and a high current carrying capability.

Semiconductor devices offer a much lower power capability, i.e. either the blocking voltage is relatively low or the maximal device current is limited. Therefore, these devices must either be connected, in series or in parallel, to achieve the same power capacityas spark-gap modulators.

However, PCD requires a high voltage for only a short time during the dischage ignition, where the current is relatively low. Thereafter, a high current is needed, but the voltage required is much lower. Consequently, the output power requirement of the modulator is much lower than the product of the maximal voltage and maximal current.

In Figure 3, a schematic of the proposed solid state modulator is shown, which is capable of generating the required high ignition voltage and the high current. The proposed topology consists of an input capacitor C_1, which provides the energy for the discharge, a semiconductor switch S_1, a pulse transformer Tr_1, a decoupling capacitor C_2 and the two saturable inductors L_{HC} and L_{MPC}. Here, an IGBT is shown for S_1 but a pulse thyristor could be applied, which would allow for higher ignition voltages and higher output currents, as we will show in section 4.

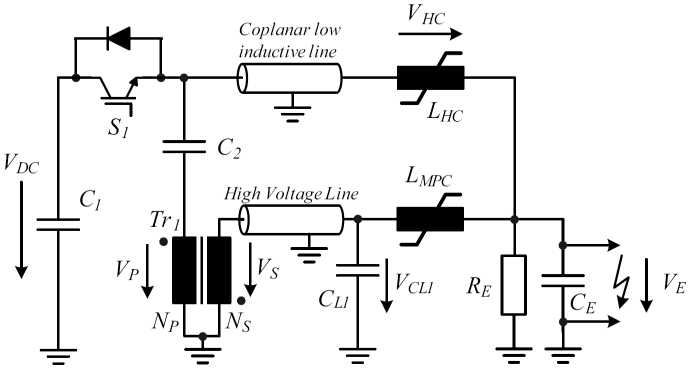

Figure 3. Schematic of the proposed pulse modulator for PCD.

2.1 OPERATING PRINCIPLE

In the following the operating principle of the solid state modulator for PCD is explained. At the beginning, switch S_1 is open and capacitor C_1 is charged up to V_{DC}, andcapacitors C_2, C_{L1} and C_E are completely discharged. Capacitor C_{L1} is in the range of a few 100 pF and is realised by the high-voltage coaxial line. The inductance of the line is considered in combination with the leakage inductance of the transformer, which is much higher. With C_E the parasitic capacitance of the electrodes/the connection cables and with R_E the resistance of the electrodes, which is mainly determined by the water, are modelled ($R_E \approx 2$ kΩ / $C_E \approx 200$ pF in the considered case).

To generate an output pulse, switch S_1 is closed and the input voltage V_{DC} is applied to the primary winding of

transformer Tr_1, since the voltage across capacitor C_2 is zero. On the secondary side, the voltage is the primary voltage V_P multiplied by N_S/N_P. If any parasitic effects are neglected, the leakage inductance L_σ of the transformer forms an LC-circuit with the parasitic capacitor C_{L1} of the line, so that the voltage V_{CL1} starts to resonate to a maximum of $2N_S/N_P$ x V_P During this time the saturable inductor L_{MPC} is not saturated yet, i.e. the LC-circuit is approximately unloaded/undamped.

Saturable inductor L_{MPC} is used in combination with the parasitic capacitor C_{L1}/C_E to perform a magnetic pulse compression, so that the rise-time of the electrode voltage V_E is decreased. The values of C_{L1} and C_E are adjusted by the connecting cables between the saturable inductors and the electrode, as well as by the electrode's shape. With the resonance of L_σ and C_{L1} as well as with the magnetic pulse compression, voltage V_E rises rapidly until a breakdown occurs. Ideally, L_{MPC} saturates when V_{CL1} is maximal, which results in a minimal rise-time and a maximal voltage V_E.

Due to the winding direction of transformer Tr_1 voltage V_E starts to rise in the negative direction, so that the voltage V_{HC} across inductor L_{HC} is positive and its core is magnetised in the positive direction. The saturation current and the maximal possible flux of L_{HC} must be chosen so, that L_{MPC} saturates before L_{HC}, i.e. L_{HC} must saturate shortly after the breakdown. During the rise of V_E until the breakdown, inductor L_{HC} blocks the high pulse voltage and the coplanar low-inductive connecting line between the switch S_1 and L_{HC} is charged to the input voltage V_{DC}.

At this point the breakdown the voltage V_E rapidly decreases and a thermal plasma is created by the current flowing from the transformer and the stored energy in C_{L1} and C_E. The voltage across L_{HC} is still positive, so that the core is further magnetized in the positive direction. This isneeded to achieve a rapid breakdown after the saturation of L_{HC} and to avoid extinguishing the arc. Consequently, shortly after the breakdown, inductor L_{HC} saturates and connects the input capacitor C_1 via switch S_1 to the electrodes, resulting in an inversion of V_E and the arc current. Due to the relatively large time constants of the charge in the plasma, the arc is not extinguishing during the rapid inversion (cf. e.g. resonant operation of HID lamps).

The connection between S_1 and L_{HC} is made of low inductive coplanar conductors, so that the current to the electrodes can rise rapidly. In order to minimise the parasitic capacitance of the electrodes, which must be charged by the high voltage ignition pulse, inductors L_{HC} and L_{MPC} are placed as close as possible to the electrodes. The parasitic capacitance of the two saturable inductors is minimized by limiting the number of turns. The arrangement of the electrodes/modulator is shown in section 3, where the 3D setup of the modulator is explained.

After L_{HC} saturated the energy stored in C_1, C_2 and C_{L1} is transferred to the arc and the plasma channel is rapidly expanding due to the increasing temperatures. As soon as the energy is transferred to the output and the capacitors are discharged, switch S_1 is opened and input capacitor C_1 is charged again, so that the modulator is ready for the next pulse.

2.2 MODULATOR WITH PULSE THYRISTOR

In order to generate the peak output voltages required for ignition, a 4.5 kV pulse thyristor could be used instead of the Insulated Gate Bipolar Transistor (IGBT). With this device the maximal input voltage is 2.8 kV and the maximal achieveable ignition voltage with the considered pulse transformer is higher than 90 kV. The peak output current is 11 kA as could be seen in Figure 11, which shows the simulation results for the thyristor modulator. The breakdown, which is assumed to happen at 90 kV, is shown in detail. Because of the larger charging current of the parasitic capacitors at the electrodes and the increased input voltage, the rise-time of the output voltage reduces to 20 ns. A 3D mechanical drawing of the modulator based on the pulse thyristor 5SPR 26L4506 made by ABB is shown in Figure 4. The overall dimensions are 50 cm × 30 cm × 20 cm, which is not much bigger than the system with the IGBT.

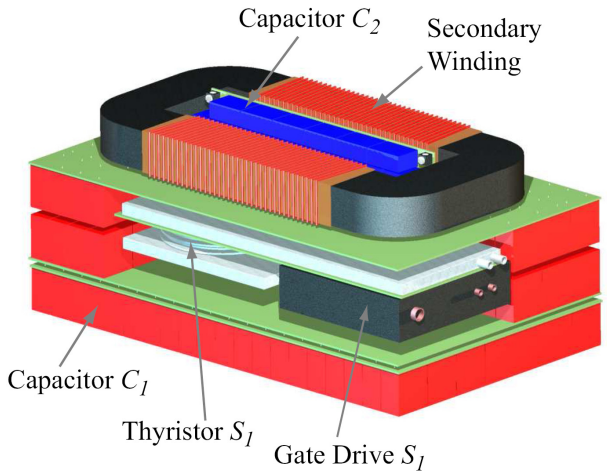

Figure 4. 3D mechanical drawing of the solid state modulator based on the pulse thyristor 5SPR 26L4506 – Dimensions: 50 cm x 30 cm x 20 cm.

3 TEST SETUP

In order to validate the concept presented in section 2 a prototype setup with the components given in Table 2 has been built. In Figure 5 a photo of the prototype is given, where the input capacitor C_1, the IGBT S_1, the decoupling capacitor C_2 and the step up transformer Tr_1 are shown. In order to minimize/control the leakage inductance of the transformer two parallel connected single turns on the two legs of the U-core are used as primary winding and the secondary is made of two windings consisting of two series connected $N_s/2$ turns. The high output voltage is fed via four parallel connected RG-213 lines to the saturable inductors L_{MPC}. There, the cable capacitance and the parasitic inductances build a resonant circuit resulting in a resonance of V_{CL1}, so that this voltage becomes higher than V_P x N_S/N_P, what results in a higher ignition voltage.

Parallel to decoupling capacitor C_2 three high voltage capacitors C'_2 are shown in Figure 5, which allow a variation of the capacitance value of C_2 for test purposes. The high current output is made of two parallel connected copper foils in order to minimize the leakage inductance/parasitic

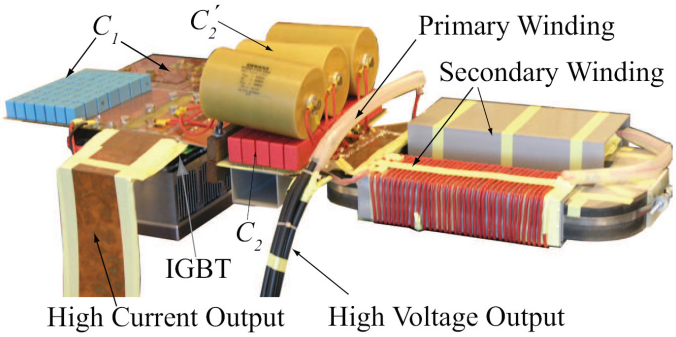

Figure 5. Photo of the prototype system for proof of concept.

capacitnace and allow a fast rising time of the current after ignition. The impact of the parasitics caused by the foils on the output voltage is small, since the capacitor is decoupled from the output by L_{HC} during the ignition.

The saturable inductor L_{HC} is made of two parallel saturable inductors, each made of 6 stacked T60006-W424 toroidal cores and two turns of litz wire. The overall dimensions of the setup is 100 mm × 50 mm × 100 mm. Inductor L_{MPC} consists of two serially connected inductors each made of 5 stacked T60006-W424 cores with 5 turns, resulting in a total size of 100 mm × 50 mm × 120 mm for L_{MPC}. By using a premagnetising circuit the number of required cores could be approximately halved. This would also guarantee that the cores are completely demagnetised after each pulse, but within the exeriments this never proved necessary.

For the pulse transformer a core made of 2605SA1 Metglas is used, which has the dimensions 41 cm × 27 mm × 9.5 cm. This core is slightly oversized, but has been chosen in order to reduce losses and enable wider variation of the input voltage for test purposes.

In a final application, the system design could be made more compact as shown in Figure 6. The modulator has a size of 50 cm × 30 cm × 12 cm and the saturable inductors approximately of 100 mm × 100 mm × 120 mm. By increasing the length of the high current and the high voltage

Table 2. Components and system parameters of the prototype pulse modulator shown in Figure 5.

Switch S_1	FZ3600R17KE3_B2 IGBT 3.6 kA/1.7 kV (Eupec)
Capacitor C_1	57 µF / 1600 V FKP4 (WIMA)
Capacitor C_2	2 µF / 2000 V FKP1 (WIMA)
Pulse Trans-former Tr_1	1:70 / 2605SA1 (Metglas) $L_\sigma \approx 100$ µH
Inductor L_{HC}	2 turns on 2 parallel 6 stacked T60006-L2040-W424 (VAC)
Inductor L_{MPC}	5 turns on 2 series 5 stacked T60006-L2040-W424 (VAC)
Parasitic R_E	≥ 400 Ω
Parasitic C_E	≤ 90 pF

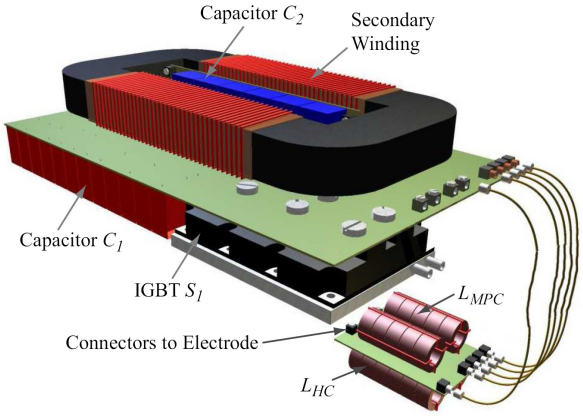

Figure 6. 3D mechanical drawing of the solid state modulator – Dimensions: 50 cm x 30 cm x 12 cm.

connecting cables, it is possible to place the modulator at some distance to the drilling electrode, so that the modulator is not directly influenced by the harsh environment of the drill head.

The electrode configuration is shown in Figure 7. The coaxial setup has an interelectrode distance of 4 mm. This distance and the geometry of the electrode determine the values of R_E and C_E in Figure 3. A similar configuration for the electrode was used in [7].

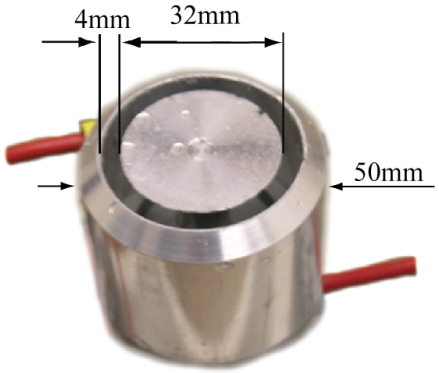

Figure 7. Coaxial electrode configuration with an interelectrode distance of 4 mm utilized in combination with the prototype in Figure 5 for the measurements shown in Figure 10 .

4 LOAD VOLTAGE/CURRENT

Based on the 3D construction in Figure 6 and the prototype given in Figure 5 the parasitic elements of the modulator system have been calculated/measured (Table 3) and a simulation including the influence of the parasitic elements has been performed (Figure 8). The leakage inductance and parasitic capacitances of the pulse transformer and the interconnection, as well as parasitic resistors have been included. Moreover, the parasitic inductances and resistances of switch S_1 and of the two capacitors C_1 and C_2 , as well as the parasitics of the saturable inductors (determined by impedance measurements), have been considered.

The simulated voltage and current waveforms under load, and the IGBT current are given in Figure 9, where it has been assumed that a breakdown occurs at 45 kV. The rise-time for

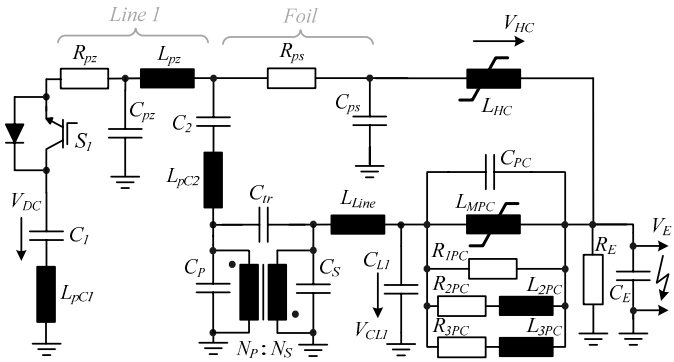

Figure 8. Schematic of the simulation circuit, which has been implemented in Simplorer.

Table 3. Parameters of the simulation circuit shown in Figure 8 .

C_1	C_1	=	50.78 µF	L_{pC1}	=	0.5 nH
C_2	C_2	=	2.04 µF	L_{pC2}	=	1 nH
Line 1	R_{pz}	=	50 mΩ	L_{pz}	=	20 nH
	C_{pz}	=	20 nF			
Foil	C_{ps}	=	10 nF	R_{ps}	=	115 µΩ
Transf.	C_P	=	50 pF	C_S	=	150 pF
	C_{tr}	=	30 pF	N_P:N_S	=	1:70
Transf. Eq. Circuit	$L_{\sigma,Sec}$	=	65 µH	$L_{h,Sec}$	=	12.6mH
	R_{Prim}	=	0.5 mΩ	R_{Sec}	=	100 mΩ
	$R_{Fe,Sec}$	=	49 kΩ			
Coax	L_{Line}	=	40 nH	C_{L1}	=	320 pF
Load	C_E	=	200 pF	R_E	=	2 kΩ

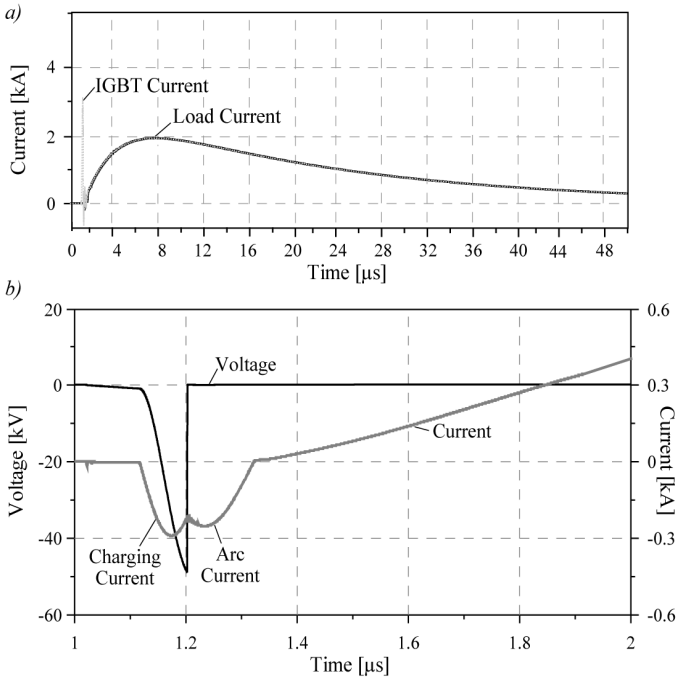

Figure 9. Simulated load and IGBT current of the modulator based on the components listed in Table 3. In (b) a zoomed view of the current in the load around the breakdown is shown, with load voltage is included.

the 45 kV is approximately 50 ns, which can be seen in Figure 9b and peak current through the arc is 2 kA. After ignition, the current through the IGBT is approximately the same as the load current, since the current flowing via the transformer/C_2 is negligible for properly selected values of C_2.

During the rising edge of the output-voltage before breakdown, the parasitic capacitance C_E is charged.After breakdown, C_E discharges via the arc and the current flows through the plasma. In the pulse after the magnetic switch L_{HC} is closed, approximately 75% of the energy stored in C_1 is transferred to the arc/output.

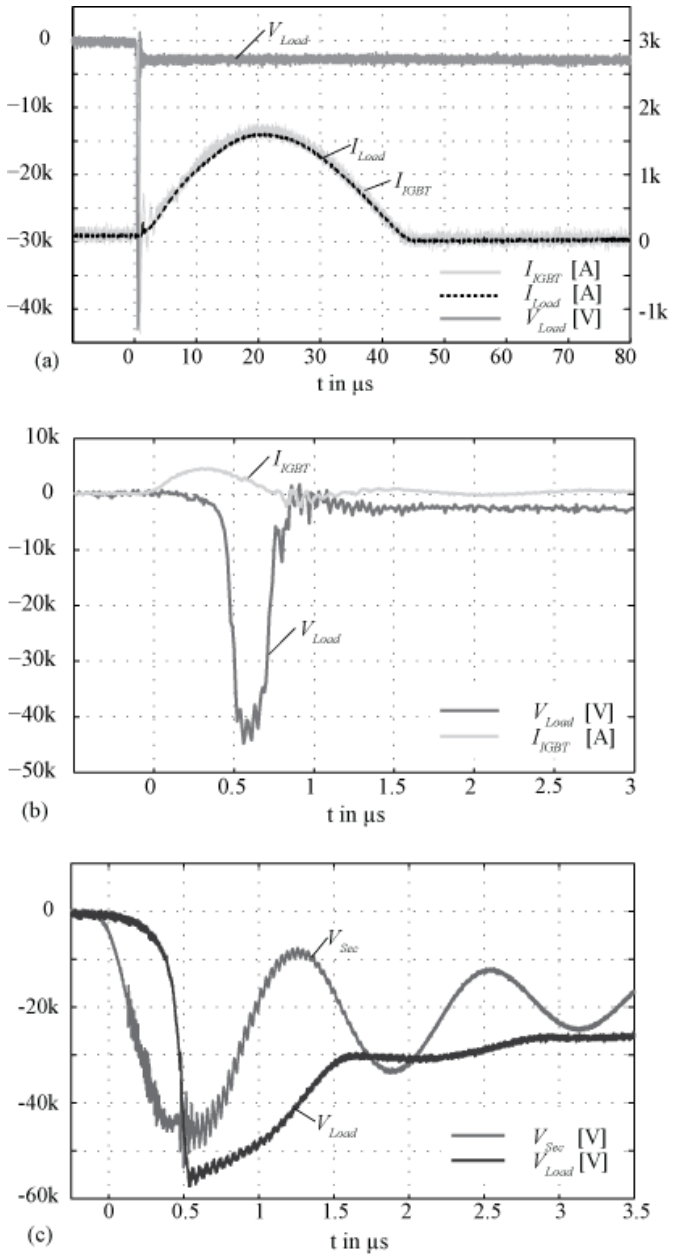

Figure 10. (a) Load voltage and IGBT current measured with the test setup and an input voltage of 1 kV. (b) Zoomed view of the ignition moment, where the rapid rise of the load voltage could be seen. (c) Secondary voltage of the transformer and output voltage, which show the saturation behaviour of L_{MPC} which results in a very fast rising edge of the load voltage. All mesurements were performed in deionized water with an interelectrode distance of 4 mm (Figure 7) and sand stone.

In Figure 10 measurement results for the test system shown in Figure 5 are given. In Figure 10a the output voltage and the IGBT current (≈ load current) are shown for a discharge occurring at approximately 45 kV in deionized water with the electrode shown in Figure 7 and sand stone. After ignition the current begins to rise, and peaks at approximately 2 kA after 20 µs. In Figure 10b a zoomed view of the moment of ignition shows that the voltage rises in less than 200 ns to its peak value. This high dv/dt is achieved with the saturable inductors as seen in Figure 10c. The secondary voltage has a relatively slow slope, which is blocked by the saturable inductors. These inductors saturate when the secondary voltage reaches its peak value and result in a fast rising edge. Due to the resonance of the parasitic elements the output voltage is higher than the secondary voltage.

In case no discharge happens, the output voltage rings up to its maximum negative peak voltage of approximately 50 - 55 kV and then resonates back to its positive peak value, which is approximately 20 kV. Thereafter, the ringing rapidly decays. Since no energy is dissipated in the load, the voltage V_{DC} across the input capacitor only slightly decreases and as soon the switch is opened capacitor C_2 and the parasitic capacitors discharge in approximately 5 ms, so that the modulator is ready for the next pulse. A 300 kΩ resistor parallel to C_2 is required for discharging, which generates roughly 50 µJ losses per pulse in normal operation. With the output voltage in the range of 50 kV, electrodes with a distance in the range of approximately 4mm can be utilized. For larger distances higher ignition voltages are required, which could be generated with the pulse thyristor based system for example. Basically, the repetition rate of the presented modulator could be in the range of a few 100 Hz, depending on the cooling of the semiconductors/magnetic components and charging of the input capacior. However, according to [3] the drilling efficiency will significantly reduce for repition rates higher than a few Hz due to the recovery time of the liquid. During the recovery time the occuring gas bubbles have to be removed. Otherwise these bubbles decrease the dielectric strength of the liquid and the breakdown will happen in the liquid and not in the rock.

Table 4. Loss energy distribution of the solid state modulator prototype system shown in Figure 5 for a single pulse.

Switch S_1	< 0.45 J
Inductor L_{MPC}	< 1.2 J
Inductor L_{HC}	< 0.4 J
Pulse transformer Tr_1	< 0.2 J

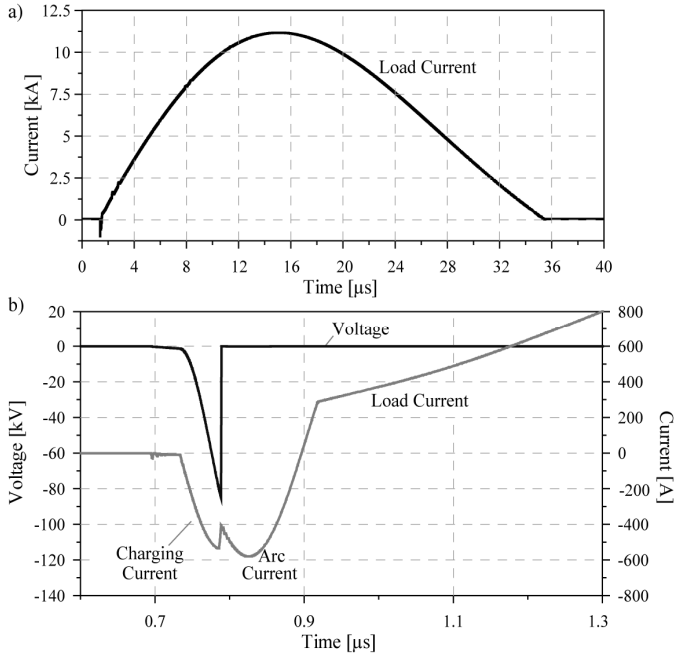

Figure 11. Load current of the modulator based on a pulse thyristor (e.g. 5SPR 26L4506 made by ABB). In (b) the zoomed view of the voltage and current waveforms around the breakdown are shown.

5 CONCLUSION

In this paper a concept for a solid state modulator which generates ignition voltages up to 45 kV and a peak output current of 2 kA for application in plasma channel drilling was presented. The modulator is based on a single semiconductor switch, two capacitors, two saturable inductors, and a pulse transformer. The operating principle, the design criteria of the pulse modulator, and the mechanical construction of a prototype have all been explained in detail. Furthermore, simulation results for the ignition voltage at the electrodes and the current through the plasma are shown, and the efficiency and the loss distribution of the system were presented. Measurement results validating the simulation results and prooving the concept have also been shown.

Furthermore, a second modulator utilizing a pulse thyristor was presented, which is capable of generating the higher output voltages and currents required for industrial PCD applications. This modulator is capable of generating ignition voltages up to 90 kV and peak output currents in the range of 11 kA.

REFERENCES

[1] A.A. Vorobiev and G.A. Vorobiev, "Electric Breakdown and Destruction of Solid Dielectrics", Vyshaya Shkola Moscow, 1966 (in Russian).

[2] B.V. Semkin, A.F. Usov and V.I. Kurets,"The Principles of Electric Impulse Destruction of Materials", Nauka, St. Petersburg, 1995 (in Russian).

[3] H. Bluhm, W. Frey, H. Giese, P. Hoppe, C. Schultheiß and R. Straßner, "Application of Pulsed HV Discharges to Material Fragmentation and Recycling", IEEE Trans. Dielectr. Electr. Insul., Vol. 7, pp. 625-636, 2000, Page(s):625 - 636.

[4] E. Linß and A. Mueller, "High performance sonic pulses - a new method for crushing of concrete", Intern. J. Mineral Processing, Vol. 74, Supplement 1, pp. 199-208, 2004.

[5] M. Neubert, *Natursteinbearbeitung mit der Elektro-impulstechnologie*, Wissensportal: Baumaschine.de, 2002.

[6] W.M. Moeny, "Method of Drilling using Pulsed Electric Drilling", U.S. Patent 2007/0137893A1, 21 June, 2007.

[7] I.V. Timoshkin, J.W. Mackersie, and Scott J. MacGregor, "Plasma Channel Miniature Hole Drilling Technology", IEEE Trans. Plasma Sci., Vol. 32, pp. 2055–2061, 2004.

[8] A.F. Usov and V.A. Tsukerman, "Electric Pulse Process for Processing of Mineral raw Materials: Energy Aspects", XXII Intern. Miner. Process. Congress, Turkey, Istanbul, pp. 714-720, 2006.

[9] G.N. Woodruff, "Low Voltage Spark Drill," U.S. Patent 3,708,002, 2 January 1973.
[10] G. Kunze and E. Anders, "Experimental Determination of the Parameters for Electrocrushing of Rock (in German)", Wissensportal www.baumaschine.de, 3(2007).
[11] W.C. Maurer, *Novel Drilling Techniques*, 1st Edition, Pergamon Press Ltd., 1968.
[12] W.C. Maurer, *Advanced Drilling Techniques*, 1st Edition, The Petroleum Publishing Company, 1980.
[13] I.V. Lisitsyn, H. Inoue, I. Nishizawa, S. Katuski and H. Akiyama, "Breakdown and Destruction of Heterogeneous Solid Dielectrics by Short High Voltage Pulses", J. Appl. Phys., Vol. 84, pp. 6262-6267, 1998.

Juergen Biela (S'04-M'06) received the diploma (with honours) from the Friedrich-Alexander University in Erlangen, Germany in 2000 and the Ph.D. degree from ETH Zurich in 2005, all in electrical engineering. In the course of M.Sc. studies he dealt in particular with resonant DC-link inverters at the Strathclyde University, Scotland (term project) and the active control of series connected IGCTs at the Technical University of Munich (diploma thesis).

He has worked at the research department of A&D Siemens, Germany, from 2000 to 2001, where he focused on inverters with very high switching frequencies, SiC components and EMC. In July 2002, he joined the Power Electronic Systems Laboratory (PES), ETH Zurich for working towards his Ph.D. degree concentrating on optimized electromagnetically integrated resonant converter. From 2006 to 2007 he was a Post-Doctoral Fellow with PES and has been a guest researcher at the Tokyo Institute of Technology, Japan. Since 2007 he is working as Senior Research Associate at PES.

His current research interest include multi-domain modelling, design and optimization of power electronic systems, in particular systems for future energy distribution and pulsed power applications, advanced power electronic systems based on novel semiconductor technologies and integrated passive components for ultra compact and ultra efficient converter systems.

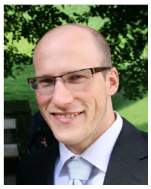

Christoph Marxgut studied electrical engineering at the University of Technology, Vienna, Austria, focusing on control systems and measurement technology. During his studies he focused on energy technology and power systems at the Swiss Federal Institute of Technology (ETH Zurich). In his Master thesis, which he wrote at the ETH Zurich, he worked on modulator design for pulsed power systems.

Dominik Bortis (S'06) was born in Fiesch, Switzerland on 29 December 1980 He studied electrical engineering at the Swiss Federal Institute of Technology (ETH) Zurich. During his studies he majored in communication technology and automatic control engineering. In his diploma thesis he worked with the company Levitronix, where he designed and realised a galvanic isolation system for analog signals. He received his M.Sc. degree in 2005, and he has been a Ph.D. student at the Power Electronic Systems Laboratory, ETH Zürich, since June 2005.

Johann W. Kolar (M'89-SM'02) studied industrial electronics at the University of Technology Vienna, Austria, where he also received the Ph.D. degree (summa cum laude). From 1984 to 2001 he was with the University of Technology in Vienna, where he was teaching and working in research in close collaboration with industry. He has proposed numerous novel converter topologies, e.g., the VIENNA Rectifier and the Three-Phase AC-AC Sparse Matrix Converter concept. Dr. Kolar has published over 300 scientific papers in international journals and conference proceedings and has filed more than 75 patents. He was appointed Professor and Head of the Power Electronics Systems Laboratory at the ETH Zurich in 2001.